https://doi.org/10.1016/j.apenergy.2019.04.162

Integration of reversible solid oxide cells with methane synthesis (ReSOC-MS) in grid stabilization: a dynamic investigation

Bin Chen[1,2,4], Yashar S. Hajimolana[2,3,*], Vikrant Venkataraman[2], Meng Ni[4,*], P.V.Aravind[2]

[1] Institute of Deep Earth Sciences and Green Energy, Shenzhen University, Shenzhen 518060, China

[2] Process and Energy Department, Delft University of Technology, Leeghwaterstraat 44, CA Delft 2628, The Netherlands

[3] Department of Thermal and Fluid Engineering, Faculty of Engineering Technology, University of Twente, Drienerlolaan 5, 7500 AE Enschede, The Netherlands

[4] Building Energy Research Group, Department of Building and Real Estate The Hong Kong Polytechnic University, Hung Hom, Kowloon, Hong Kong, China

Abstract

The power to gas process concept is promising for the next generation of electronical energy storage and grid stabilization technologies. The electricity-driven fuel production can be chosen to be the efficient energy carrier for excessive grid power. Here, a reversible solid oxide cells system integrated with methane synthesis (ReSOC-MS) is proposed for the grid stabilization application at Mega Watts class. Besides H_2, CH_4 can be inclusively synthesized at grid surplus conditions as a transportation friendly energy carrier. A control strategy is proposed for this combined system, based on the grid state and H_2 tank state of the system for the normal solid oxide fuel cell (SOFC) mode and solid oxide electrolysis cell (SOEC) mode. Simulation results of these two operational modes demonstrate that the ReSOC-MS can achieve an 85.34% power to gas efficiency at SOEC mode and 46.95% gas to power efficiency at SOFC mode. Dynamic simulations of stepping grid state for 5000 seconds operation show that the power to gas efficiency can be higher than 70%, successfully demonstrating the capability of grid-balancing and methane production.

Keywords: Reversible solid oxide cell; Methane synthesis; Grid stabilization; Hydrogen storage; Dynamic simulation; Power control strategy; Power-to-X

The short version of the paper was presented at ICAE2018, Aug 22-25, Hong Kong. This paper is a substantial extension of conference paper.

[*]Corresponding author:
Email: s.hajimolana@utwente.nl (Yashar S. Hajimolana),

Tel: +31 534898462
bsmengni@polyu.edu.hk (Meng Ni)
Tel: +852 27664152

Highlights

A novel reversible solid oxide fuel cells system for grid stabilization.
A two-staged methanation subsystem utilizes the H_2 from SOEC operating and CO_2.
A control strategy of 7 modes (**M1**–**M7**) operation is proposed.
M2 and **M6** are optimal in terms of energy efficiency and system risk.
Dynamic simulations are conducted to investigate the system.

1 Introduction

Alternative energy sources are urgently demanded to limit global warming bellow 1.5°C, avoiding environmental degradation. Renewable energy sources (RESs) like wind, tidal and solar energy can provide sustaining power in an eco-friendly way [1]. However, RESs are usually intermittent, unstable and seasonal-changing. The characteristics make the integration of RESs into the grid more challenging and propose a need for energy storage. Therefore, balancing the power grids with a suitable balancing power plant that can effectively overcome the shortcoming of the renewable sources is necessary. Grid energy storage technologies can be categorized as electrochemical methods (battery, capacitor), mechanical methods (compressed air, flywheel) and thermal storage [2], which are required to have high roundtrip efficiency, low capital cost and fast response [3]. Reversible Solid Oxide Cell (ReSOC) system is a promising technology which can effectively turn surplus power into H_2, CO and O_2 (electrolysis mode) and produce power by reverse process (fuel cell mode). The system that can operate in both solid oxide electrolyser (SOEC) and solid oxide fuel cell (SOFC) mode potentially allows the reduction of complexity, carbon footprint and cost of the Power-to-X plant, unifying hydrogen production and utilization in the same device. In this regenerative operating mode, SOFC/SOEC system is able to better utilize and support electricity grid. One main technical obstacle in using ReSOC for grid stabilization is the H_2 storage at the SOEC operational mode. Finding a cost-effective method of storing H_2 remains a difficult challenge [5]. An alternative strategy is the further conversion of H_2 at SOEC mode to methane, methanol or other hydrocarbon productions that are friendly for store and transportation [6].

Jensen et al. proposed a methane synthesis system by internal reforming H_2 and CO in ReSOC, followed by underground storage of pressurized CH_4. Analysis of the system reveals that ReSOC is thermodynamically and economically benign for high-efficiency large scale electricity storage [7]. Wendel et. al. studied the thermal management and operating conditions for a pressurized ReSOC system with internal methane production (CO methanation), finding a 70% roundtrip efficiency at elevated operating stack pressure (20 bar) [8]. Tinoco et al. investigated a catalytical H_2 to methanol process at 80 bar, 533 K, at which the H_2 can react with CO_2 to produce liquid methanol using a dynamic

simulation approach. The process is based on a CO_2/H_2 co-electrolysis SOEC and a single-step methanol reactor [9].

Compared to the CO methanation mentioned above, CO_2 methanation is considered as a more attractive option since it can serve to recycle the CO_2 from various carbon capture and storage (CCS) technologies. By this, CO_2 emission can be alleviated by increasing the penetration of as-synthesized sustainable methane into the fuel supply chain. Besides, CO_2 methanation can also be operated at moderate conditions in well-commercialized large scale methanators, which use low-cost Ni-based catalysts, e.g. the adiabatic fixed bed process system from Lurgi GmbH and TREMP^{TM}, cooled fixed-bed from Linde, and other fluidized-bed methanation processes [10].

Therefore, this paper proposes a system with the reversible solid oxide cell subsystem and the methane synthesis subsystem (ReSOC-MS) for the grid power stabilization. At the SOEC mode, the ReSOC-MS system can utilize surplus electricity from the grid to produce H_2, which, optionally, can be further used for CO_2 methanation as a form of grid electricity storage. At the SOFC mode, ReSOC-MS generates electricity from stored H_2 so to stabilize the grid. To simplify the system, the two subsystems are thermally coupled to recycle waste heat and to regenerate steam so that external supplying of steam and heat can be spared to a great extent. Further, a preliminary control strategy for the combined system is proposed to ensure the stabilization of the grid and the system.

2 Model development

2.1 Overview of the system

The ReSOC-MS system consists of two sub-systems as depicted in **Fig. 1**: the ReSOC subsystem and the methanation subsystem, connected by the H_2 supply stream (***S16***) and the water recycle stream (***S18***). The grid is linked to the ReSOC subsystem by the electricity output (W_{elec_EC} in the unit of MW) to the ReSOC. When there is an electricity surplus in the grid, the excess electricity stores by the ReSOC subsystem at SOEC operational mode. Alternatively, during electricity shortage, the grid is connected to the ReSOC by the electricity input (W_{elec_FC}), thus the ReSOC operates at SOFC mode to

generate the electricity demand from the grid. A proper PID controller is employed to regulate the power of ReSOC by manipulating the current density.

Steam electrolysis at 600 °C for producing H_2 and O_2 from steam at SOEC mode:

$$2H_2O = O_2 + 2H_2 \qquad \Delta H = 493 \text{ kJ mol}^{-1} \tag{1}$$

Regarding the accumulated electricity surplus from fluctuating grid, the stored H_2 in the tank may exceed, therefore, it needs to be further transferred to the methane synthesis subsystem for the Sabatier reaction:

$$CO_2 + 4H_2 = CH_4 + 2H_2O \quad \Delta H = -164 \text{ kJ mol}^{-1} \tag{2}$$

The methane synthesis subsystem consists of two Sabatier reactors with inter-stage cooling. The H_2 sources from the H_2 tank would be firstly adiabatically compressed to the working pressure (10 bar, ***S17***), and mixed with the compressed CO_2 (***S19***) source and the recycled product gas (***S26***). The inlet gas temperature of the first stage Methanator1 is fixed at 250°C by means of gas recycle from Condenser ***C2***. To improve the conversion of CO_2 and H_2 to CH_4, the steam generator (***SG1***, an evaporative water intercooler) is used to lower down the temperature of ***S21*** to 400°C, while the steam (***S22***) generated from the evaporation of water can be used as the reactant of the electrolysis process ongoing at the ReSOC (SOEC mode). The CH_4 is to be furtherly synthesized in the Methanator2 with the waste heat of the off-gas (***S23***) recuperated by the steam generator (***SG2***), meanwhile yielding steam (***S25***). Finally, the condenser ***C2*** will condense the steam contained in ***S24*** to liquid water (***S18***) and then the CH_4 rich gas (***S27***) is stored with 10% recycled to Methanator1.

As said, the control bus component is responsible for the real-time control of gas streams flux so that the ReSOC-MS system can switch between SOFC mode and SOEC mode. To achieve this, the system state should firstly defined by two descriptive variables: the grid state S_e and the H_2 tank state S_{H_2}. The dimensionless S_e represents the grid electricity surplus or shortage, normalized to 5 MW ($E_{nominal}$) from -1.0 to 1.0 in the tentative application scenario:

$$S_e = \frac{-W_{elec\_EC}}{E_{nominal}} \, or \, \frac{W_{elec\_FC}}{E_{nominal}} \tag{3}$$

The other state variable is S_{H_2}, representing the filling degree of the H_2 tank:

$$S_{H_2} = \frac{Volume\ of\ H_2\ \text{stored}}{Maximum\ volume\ of\ H_2\ tank} \quad (4)$$

Evidently, S_e is negative when the grid is subject to the electricity demand, which is less than the supply, implying that redundant electricity needs to be stored via electrolysis process (SOEC mode). When S_e is larger than zero, the ReSOC would be operated at SOFC mode to compensate the electricity shortage, thus securing the grid balance. It is assumed than the upper bound of fluctuating renewable power plant grid (W_{elec_EC} or W_{elec_FC}) is less than E_nominal in all scenarios, so that the intermittence of the grid can be mimicked by the changing S_e within ±1 as a simplification. The other state variable is S_{H_2}, representing the filling degree of the H_2 tank from 0% to 100% filled. A state-dependent control strategy based on these two state variables is implemented into the control bus to regulate three pipe opening valves (***V1***-***V3***). The details of the control strategy are referred to the Section 2.4.

To investigate the efficiency and dynamic operation of the proposed system, the system model is developed in the dynamic simulation Platform OpenModelica based on the process modelling language Modelica. Using the built-in basic blocks of OpenModelica, models for system components are developed and connected, with 5590 variables to be solved using the DASSL dynamic solver with a 0.02s time step. The computational time for a simulated 5000s operation is less than 5 min. The following section will introduce the details of component model development.

2.2 ReSOC subsystem model

The ReSOC subsystem utilizes redundant electricity (W_{elec_EC}) from the grid to electrolyze the steam-rich stream (***S9***, the mixture of ***S6***, ***S22***, ***S25*** and ***S28***) to produce H_2 and O_2. The electricity-powered steam generator (***SG3***) is responsible for supplying additional steam to adjust the fraction of steam in ***S9*** before entering the stack. The fuel stream (***S7***) is heated up to the operating temperature (600 °C) by heat exchanger ***HX1*** and heater ***H1***. The produced H_2 by ReSOC (SOEC mode) in ***S10*** is stored in the H_2 tank via ***S14***, after proper heat recuperation (at ***HX1***) and unused steam splitting at Condenser (***C1***). The stored H_2 can be utilized by the ReSOC via ***S28*** to generate electricity, thus avoiding the grid shortage when the ReSOC operates at SOFC mode (reserved **Eq. 1**). The storage of H_2 at the storage

tank is assumed to be ideal, without thermal loss/leakage during the operation. Low-pressure absorption method, e.g. using metal hydride is assumed for this H_2 storage tank [11,12], mainly for two reasons: firstly, the ReSOC stack is intended to operate under ambient pressure as a high-pressure operation will inevitably bring complexity to the ReSOC subsystem, although it is thermodynamically beneficial in terms of energy efficiency; secondly in the reversible ReSOC system, compressed storage of H_2 will require additional compressing/expansion work for H_2 so that significant energy loss will be accompanied. The H_2 balance at the H_2 storage tank is controlled by three valves (***V1***, ***V2*** and ***V3***), which are regulated by the control bus. It should be noted that ***V1*** is a bidirectional valve for H_2 exporting/replenishing, assuming that its opening can be two-way, i.e. −1 to 0 for exporting and 0 to +1 for replenishing, to avoid the overfilling and exhausting of the H_2 storage tank.

On the air electrode side, the air flow rate is 0.5 mol s^{-1} at SOEC mode as the carrying gas supplied by the compressed air tank. At SOFC mode, the air flow is proportional to S_e, i.e. $10 \cdot S_e$ mol s^{-1} so that the utilization of the oxygen is controlled at 30%. The offgas from air channel at SOEC mode is oxygen-rich, thus is stored in the O_2 rich gas storage tank as a chemical production. Heat exchanger ***HX2*** and Heater ***H2*** are also designed to control the inlet temperature of the air flow stream (***S3***) to be consistent with that of the inlet fuel flow of the ReSOC. The ***HX1*** and ***HX2*** are counter-flow type with the effectiveness factor at 0.85. The effectiveness factor is defined as the ratio of the actual heat exchange rate to the theoretical maximum heat exchange rate between the two fluid streams [13]. Table 1 summarized the operating parameters for the blocks in the ReSOC subsystem.

A zero-dimensional dynamic model for the stack is developed based on transfer functions of the partial pressure of participating gas species. Ohmic loss, activation loss and concentration loss are all taken into consideration in this model. The transfer function based zero-dimensional dynamic model has advantages in integrating with system control algorithms, compared to traditional numerical models (e.g. Finite Element Method, Finite Volume Method) that require time-consuming computational solving of partial differential equations. **Fig. S1** shows the mathematical model of the stack with three input ports and three output ports interfaced to external components in the ReSOC system [14,15]. The first input port is the operating current density instructed by the PID controller, and the

other two are the fuel inflow stream and air inflow stream. The power output port is connected to the PID controller for the current control, while the fuel output and air output port are connected to other components for further heat recover and gas processing as shown in **Fig. 1**. The grid state parameters (electricity input W_{elec_FC} to ReSOC; or W_{elec_EC} output from ReSOC) are used as the "setpoint" of the PID controller. The "error value" is the difference between stack power and the "setpoint". The operating current of the stack is the manipulated variable by the controller. The controller will fail when the grid power is beyond the power capacity of the stack, which is defined as W_{elec_FC} > 1.28 MW and W_{elec_EC} > 6.4 MW. The PID coefficients *kp*, *ki* and *kd*, representing the proportional, integral and derivate gains, were manually tuned to ensure that the output power from the stack can response to the grid state without oscillating, referred to **Table 1**.

The following are assumptions used in this ReSOC model:

1. All gas flows behave as ideal gases.
2. The temperature of the ReSOC is set as the inlet temperature 600 °C.
3. The gas channel is a fixed control volume and the flow is assumed to be plug flow.
4. The Nernst equation is applied to calculate the open circuit voltage.
5. A First-order transfer function is used to describe the gas composition change during the process.
6. The two flows of channels are choked at orifices of outlets [16].

Using the models and assumptions mentioned above, the finial zero dimensional dynamic ReSOC stack model is implemented with other components to form the ReSOC subsystem. **Fig. 2** shows the simulated current-voltage curve of a single cell of the ReSOC stack, that is a conservative representative of current solid oxide cell performance at intermediate temperature (600 ^{o}C), of which the maximum power density ranging from 0.2 W cm^{-2} to 1.58 W cm^{-2} [17]. For simplicity, the single cell performance is extrapolated to represent every cell in the whole stack. The discontinuity of the current curve between the SOEC mode and SOFC mode arises from the different inlet fuel gas compositions.

2.3 Methanation subsystem

The methanation subsystem is responsible for the synthesis of methane using the H_2 stored in the storage tank (25 °C, 1 bar), which is accumulatively produced by the ReSOC subsystem at the SOEC mode. The process is based on the concept of CO_2 methanation (Sabatier reaction) in two identical adiabatic fixed-bed methanators (Methanator1 and Methanator2) with inter-stage cooling. The process proposed here is learned from the exemplary 3-staged TREMP methanation process developed by Haldor Topsøe™ [10].

The H_2 sources from the H_2 storage tank is firstly adiabatically compressed to the operating pressure (10 bar, ***S17***), and then mixed with the compressed CO_2 (***S19***) source and the recycled product gas (***S26***). The inlet gas temperature of the first stage Methanator1 is fixed at 250 °C by means of gas recycle from Condenser ***C2***. To improve the conversion of CO_2 and H_2 to CH_4, the steam generator (***SG1***, an evaporative water intercooler) is used to lower down the temperature of ***S21*** to 400 °C, while the steam (***S22***) generated from the evaporation of water can be used as the reactant for the electrolysis process ongoing at the ReSOC (SOEC case). The CH_4 is to be furtherly synthesized in the Methanator2 with the waste heat of the off-gas (***S23***) recuperated by the steam generator (***SG2***), meanwhile yielding steam (***S25***). Finally, the steam contained in ***S24*** is condensed to liquid water (***S18***) by the condenser ***C2*** and the CH_4 rich gas (***S27***) is stored with 10% recycled to Methanator1.

The main advantage of the methanation process proposed in this study is the byproduct steam would be recycled to the ReSOC as the reactant of H_2O electrolysis, and the heat recovery of the methanation process at the same time. The main reaction occurring in two methanators is the so-called CO_2 methanation reaction (see **Eq. 2**). As it is an endothermic reaction, a higher yield of CH_4 is favoured at the lower temperature, as shown in **Fig. 3** that the theoretical equilibrium yield of CH_4 approaches 1 when the temperature is decreasing. Therefore, the feeding gas temperature of Methantor1 are controlled at 250 °C to thermodynamically facilitate the CH_4 production. Preheating the H_2 stream and recycling 10% of the outlet gas flow of Methanator2 at the condenser (***C2***) are the two measures to control the inlet temperature of Methanator1. Before Methanator2, ***SG1*** is used to cool down the outlet gas of Methanator1 to 400 °C before entering Methanator2. The design

parameters for the methanators are summarized in **Table 2**. The operating parameters for auxiliary components of the methanation subsystem are listed in **Table 3**.

The mathematical model for CO_2 methanation reactors is based on the kinetics over Ni/Al_2O_3 catalyst, adopted from Koschany's power law equation [22].

$$r = k \cdot \frac{p_{H_2}^{n_{H_2}} p_{CO_2}^{n_{CO_2}}}{1+K_{OH}\frac{p_{H_2O}}{p_{H_2}^{1/2}}} \left(1 - \frac{p_{CH_4}\, p_{H_2O}^2}{p_{H_2}^4\, p_{CO_2}\, K_{eq}}\right) \quad (5)$$

which the r represents the volume-based reaction rate of CO_2 methanation in mol (s^{-1} m^{-3}). A one-dimensional plug-flow model is developed to simulate the reaction process inside the methanator along the flow direction [23]. The radial gradients of temperature, species concentration, the heat losses and pressure drop along the flow are neglected. By so, the spatial-dependent model can calculate the distribution of reaction rates , the temperature of the gas flow T and the gas species concentration c_j.

2.4 Control strategy

As briefly mentioned in Section 2.1, the control strategy implemented in the control bus block is to regulate ReSOC-MS system in switching between SOFC mode and SOEC mode, as well as managing the co-operating of the methane synthesis subsystem. The control strategy is based on two variables (S_e, S_{H_2}), which maps out the system state space (**Fig. 4**) that is partitioned to 7 regions, each corresponding to an operation mode (**M1**–**M7**) to improve the control performance. By this, comprehensive control strategies are implemented for incorporating the methanation subsystem with the ReSOC subsystem. Generally, **M1**–**M3** are responsible for subdividing the SOFC case operating when $S_e > 0$. Specifically, **M2** is the optimal mode for SOFC operating as the H_2 used by the SOFC is pre-stored, without the need for external supply of H_2 (e.g. **M1**) that could be more energy-costive. It is rational to activate the methanation process at **M3** to consume H_2 when the filling of H_2 storage tank is close to 100%, notwithstanding the ReSOC also needs H_2 for SOFC operating. On the other hand, **M4**–**M7** are for subdividing SOEC operating when $S_e < 0$. At **M4** and **M5**, the methanation system is designed to be inactive, considering that the stored H_2 is close to depletion. **M6** is deemed as the optimal condition since the filling of H_2 stack can be properly regulated to reduce the risk of brimming by flexibly controlling the H_2 consumption rate to the methanation process (partial activation of methanation by

V3). Therefore, the aforementioned 7 modes operating enables the proper integration of methanation subsystem to the ReSOC subsystem by controlling the openings of three valves of H_2 tank (***V1***, ***V2*** and ***V3***) to regulate the H_2 consumption/production rate, methanation rate and the exporting/replenishing of the H_2 storage tank, respectively. The maximum openings of ***V1***–***V3*** for H_2 flowrate are capped at 25 mol s^{-1}, 55 mol s^{-1} and 20 mol s^{-1}. The strategies are mathematically formulated as:

$$\mathbf{M}\left(S_e, S_{H_2}\right) =$$

$$\begin{aligned}
&\mathbf{M1}: V1 = -1(H_2\ replenishing); V2 = S_e(SOFC); V3 = 0, && S_{H_2} < 0.125; 0 < S_e \le 1\\
&\mathbf{M2}: V1 = 0; V2 = S_e(SOFC); V3 = 0, && 0 \le S_e - 2S_{H_2} + 1;\ 0.125 \le S_{H_2}; 0 < S_e \le 1\\
&\mathbf{M3}: V1 = \begin{cases} 0 & S_{H_2} < 1 \\ 1 & S_{H_2} = 1, H_2\ exporting \end{cases};\\
&\quad V2 = S_e(SOFC); V3 = 2S_{H_2} - S_e - 1(Methanation), && S_e - 2S_{H_2} + 1 < 0, 0 < S_e \le 1\\
&\mathbf{M4}: V1 = -1(H_2\ replenishing); V2 = 0.05(SOEC); V3 = 0, && S_{H_2} < 0.125; -1 \le S_e \le 0\\
&\mathbf{M5}: V1 = 0; V2 = 0.05(SOEC); V3 = 0, && S_{H_2} \ge 0.125;\ S_e - 4S_{H_2} \ge -2, -1 \le S_e \le 0\\
&\mathbf{M6}: V1 = 0; V2 = 0.05(SOEC); V3 = S_{H_2} - (S_e + 2)\ /\ 4\ (Methanation), && -4 < S_e - 4S_{H_2} < -2, -1 \le S_e \le 0\\
&\mathbf{M7}: V1 = \begin{cases} 0 & S_{H_2} < 1 \\ 1 & S_{H_2} = 1, H_2\ exporting \end{cases}; V2 = 0.05(SOEC); V3 = 1(Methanation), && S_e - 4S_{H_2} \le -4, -1 \le S_e \le 0
\end{aligned} \tag{6}$$

Using this control strategy, the system can be dynamically operated at fluctuating S_e, taking the real-time filling state of H_2 tank into consideration. To make clear, **Table S2** briefs the operating states of the ReSOC subsystem and the methanation subsystem under those seven modes. The detailed description of each mode is also introduced in the supporting information. To evaluate the robustness of the system, two stationaries S_e cases and two stepping S_e cases are conducted, for both SOEC and SOFC operation modes respectively. This will be discussed in the next section.

3 Results

3.1 Stationary results

Firstly, two stationary cases are conducted to simulate 1000 s operating at SOFC mode and SOEC mode, respectively. The stationary S_e and the initial S_{H_2} for each mode are defined as:

$$\text{SOFC case: } S_e = 0.25, S_{H_2} = 0.5 \tag{7}$$

$$\text{SOEC case: } S_e = -0.4, S_{H_2} = 0.5 \tag{8}$$

The initial H_2 storage tank state are set at 50% filled ($S_{H_2} = 0.5$). The stack in the SOFC mode ($S_e = 0.25$) is generated 1 MW of power to the grid accordingly, while at the SOEC mode, the stack is required to utilize 2 MW of power from the grid ($S_e = -0.4$) as abstracted in **Fig. 4**. The simulated change of (S_e, S_{H_2}) overtime is tracked in **Fig. 5**. In the SOFC mode, the ***V3*** is always closed as the methanation subsystem is not activated as the value of S_{H_2} is lower than 0.5. Therefore, the operation mode is at **M2** and would not enter **M3**. The S_e is kept at 0.25 since it is pre-defined to be stationary.

In the SOEC mode, the ***V3*** initially delivers H_2 (4 mol s^{-1}) from the H_2 storage tank to the methanation subsystem with its opening set at 0.2. Then, the opening of ***V3*** gradually increases to 0.292 due to the increase of S_{H_2}. The adaptive control of ***V3*** in the case of changing S_{H_2} is realized by the location mapping of (S_e, S_{H_2}) between two boundaries for ***V3*** as it can be seen in the **Fig. 4**. This strategy is expected to improve the robustness of the energy storage system by enhancement of H_2 consumption via ***V3***. That results in the increase of total methane yielding (y_{CH_4}) as observed in **Fig. 5c**. Finally, the S_{H_2} is only increased to 0.538, indicating that the current system design is competent to balance MW scale grid at the time scale of thousand seconds. The integration of methanation subsystem and the (S_e, S_{H_2})-dependent methanation rate as designed are proven to be able to mitigate the H_2 storage issue. The initial quick decay of y_{CH_4} before $t \approx 30$ s is because of the quick cooling effect of methanation reaction at the initial stage. The conversions of H_2 at each methanator (noted as $U1$ and $U2$) do not change much with the varying of ***V3***, indicating that the methanation capacity of two methanators are sufficient for converting the H_2 input, so that the flow is close to the equilibrium state at the outlet of each methanators. **Table 4** gives the performance summary of these two stationary simulation cases.

Fig. 6 compares the energy incomings and outgoings for both SOEC and SOFC modes. It should be noted that auxiliary equipment, such as compressors and heaters, need to be powered. Therefore, the total energy input as shown in **Fig. 6a** (SOEC mode), is the sum of the grid electricity towards the ReSOC and additional electricity input to auxiliary equipment. At 1000 s of SOEC mode, a total of 2.59 GJ power is delivered to the ReSOC system, of which 2 GJ is from the grid to be balanced. 0.59 GJ is from other sources for the auxiliary components. 77.35% of 2.59 GJ is utilized by the electrolysis process in the

ReSOC stack. Regarding the energy output in **Fig. 6b**, it can be seen that 14.66% of energy is wasted, 56.4% of energy is stored in the CH_4 via methanation and 28.94% of energy is stored in the produced H_2. This conversion efficiency is achieved at 1.44 V which is close to the thermal-neutral voltage (approximately 1.27 V at 600 °C [24]), neglecting the pipeline losses, heat dissipation in gas tanks and heat exchangers. At the SOFC mode (**Fig. 6c**), 97.63% (2.13 GJ) of the total energy input originates from the High Heating Value (HHV) of the consumed H_2, while a slight amount of electricity is needed for other components. Finally, the 46.95% of the total energy input is converted to the grid power (**Fig. 6d**).

3.2 Dynamic response results

To simulate the grid fluctuations, two stepping electricity conditions for the surplus and shortage are assumed, each lasting for a time span of 5000 s, represented by the stepping grid state variable S_e:

At grid electricity surplus (SOEC case):

$$S_e = \begin{cases} -0.4,\ t < 2000\ s\ (\mathrm{W}_{elec\_EC} = 2\ \mathrm{MW}) \\ -0.6,\ 2000\ s < t < 3000\ s\ (\mathrm{W}_{elec\_EC} = 3\ \mathrm{MW}) \\ -0.8,\ 3000\ s < t < 5000\ s\ (\mathrm{W}_{elec\_EC} = 4\ \mathrm{MW}) \end{cases} \quad (9)$$

At grid electricity shortage (SOFC case):

$$S_e = \begin{cases} 0.06, t < 2000\ s\ (\mathrm{W}_{elec\_FC} = 0.3\ \mathrm{MW}) \\ 0.16, 2000\ s < t < 3000\ s\ \left(\mathrm{W}_{elec\_FC} = 0.8\ \mathrm{MW}\right) \\ 0.26, 3000\ s < t < 5000\ s\ (\mathrm{W}_{\mathrm{W}_{elec\_FC}} = 1.3\ \mathrm{MW}) \end{cases} \quad (10)$$

As schemed in **Fig. 7**, the grid state value S_e in the dynamic SOEC mode (red arrows) is initially set at −0.4 for 2000 s, then decreased to -0.6 for 1000 s and is finally kept at −0.8 during the last 2000 s. The corresponding electricity inputs to the ReSOC stack (W_{elec_EC}) for the three steps are 2 MW, 6 MW and 4 MW of power, respectively. Regarding the dynamic SOFC mode, a similar stepping is applied but S_e is changed to 0.06, 0.16 and finally 0.26. **Table 5** summarizes the operation conditions and the results of SOEC operational mode. Accordingly, the dynamic operating voltage of the ReSOC is increased from 1.44 V to 1.61 V with nearly no time delay (see **Fig. 8**). Meanwhile, the H_2 storage tank is gradually filled, with the initial S_{H_2} change from 0.4 to 0.5 till *t* = 5000 s (**Fig. 9a**).

The S_{H_2} does not show step-like zigzags at stepping timepoints of S_e. This is because abrupt changing of H_2 flow (**S14**) into the H_2 storage tank is avoided, due to the opening of valve ***V3*** is controlled to be proportional to S_e, which is stepping changing. The stepping change of ***V3*** further results in the stepping of total methane production rate (y_{CH_4}) of the two methanators as seen in **Fig. 9b**. The conversion rates ($U1$ and $U2$) are stable during the whole 5000 s operating. The transient electricity storage rates (electricity to H_2 by electrolysis and electricity to CH_4 by methanation in J/s) are measured separately by the HHV value of H_2 and CH_4 in **Fig. 10a**. It can be found that the system prefers to store electricity in CH_4 at a higher degree of grid electricity surplus as CH_4 has higher volumetric energy density than H_2. The efficiency of the system (**Fig. 10b**) descends at each stepping of S_e, but still maintains above 0.7, even at 4 MW operating.

For the SOFC mode, the grid state S_e is stepped from 0.06 to 0.26 as pre-designed, represented by the green lines in **Fig. 11a**. Here it is assumed that the unbalanced amount of electricity in the SOFC mode is relatively smaller than that in the SOEC mode, because the assumed target grid for the ReSOC-MS is more often in electricity surplus conditions, i.e. powered by renewable energy resources such as wind or solar power. As it is observed, the S_{H_2} is reduced at different slopes during the three steps. From 0 s to 2000 s, ***V3*** is partially opened to deliver H_2 to the methanation process at the mode of **M3** as the storage of H_2 tank is abundant (S_e > 0.5). As seen in **Fig. 11b**, the methanation subsystem accordingly yields CH_4 production before 2000 s. Thereafter, the operating mode is switched from **M3** to **M2**, corresponding to the boundary crossing in **Fig. 7** due to the sudden change of S_e. This mode switch resulted in closing of ***V3***, due to which the production of CH_4 is stopped after t = 2000 s (see **Fig. 11b)**. After t = 3000 s, the decrease rate of S_{H_2} is constant until S_{H_2} reaches 0.125 at t = 4836 s. After that, the outsourcing mode is triggered (**M1**) that holds the S_{H_2} value at 0.125 (**Fig. 11a**). The fast responsivity of voltage and current curves of ReSOC subsystem to the step-changing S_e is illustrated in **Fig. 12a** that the operating voltage are quickly stabilized at 0.938 V, 0.776 V and 0.592 V, corresponding to the 3 grid power steps: 0.3 MW, 0.8 MW and 1.3 MW. The fuel gas to power efficiency (**Fig. 12b**) is decreased from 0.556 to 0.385 at the stepping conditions because the overpotential ought to be higher at lower operating voltage. The overall performance of SOFC operational mode is summarized in **Table 6.** A total 3999 MJ

electricity from Re-SOC at SOFC mode is supplied to the grid, achieving a 46.1% gas to power conversion efficiency. This conversion efficiency is comparable to other large-scale power generation solutions based on SOFC technologies at stationary operating around 50% [25,26]. Notably, this efficiency is achieved at the dynamic grid input conditions, during which the power generation density and the energy efficiency are traded-off by the customized valve control under the effective control strategies. This architecture of the control strategy is proven to be effective and can be further extended for more complicated reversible solid oxide cell system design.

4 Conclusions

This paper has proposed a combined system integrating reversible solid oxide cells with CO_2 methanation process (ReSOC-MS) for the grid electricity storage at a scale of MW class. A dynamic model is developed to test the capability of ReSOC-MS in grid stabilization, supervised by a dynamic control strategy based on the system state (S_{H_2}) and grid state (S_e). 7 different operating modes: **M1**–**M7**, are mapped out at different (S_e, S_{H_2}) conditions to control the ReSOC subsystem and the two-staged methanation subsystem by means of controlling the gas supply and voltage, aimed to stable fuel utilization; extending storage capacity and buffering the H_2 storage tank filling. It is shown from the simulation results of stationary tests that the power to gas efficiency of the ReSOC-MS can be achieved to 85.34% when operated at stationary grid condition (2 MW, SOEC mode at 1.44 V) with a CH_4 yield of 0.97 mol s^{-1}, viz. 68.1% CO_2 conversion ratio for 1000 s operation. At SOFC mode with 1 MW of power, gas to power efficiency of the ReSOC-MS system is achieved to 46.95% at 0.71V. In the dynamic tests of SOEC mode, it is proved that the ReSOC-MS system can store the surplus grid electricity with the power to gas efficiency above 70% if the gird surplus electricity is lower than 4 MW. The amount ratio of CH_4 production and H_2 production can be adjusted by the control strategy to extend the system capacity for grid electricity storage by refraining from storing the large volume of H_2. At the SOFC mode, the ReSOC-MS can still maintain the CH_4 production attributed when the system state is at **M3** (an acceptable level of H_2 storage).

Acknowledgments

This project BALANCE is funded by H2020 under the grant agreement 731224.

References

[1] European Union energy in figures statistical pocketbook 2017. Publications Office of the European Union; 2017.

[2] Eyer J, Corey G. Energy storage for the electricity grid: Benefits and market potential assessment guide. Sandia Natl Lab 2010;20:5.

[3] E. Hittinger, J.F. Whitacre, J. Apt, What properties of grid energy storage are most valuable? J. Power Sources. 2012;206:436–449.

[4] Zabihian F, Fung A. A review on modeling of hybrid solid oxide fuel cell systems. Int J Eng 2009;3:85–119.

[5] Niaz S, Manzoor T, Pandith AH. Hydrogen storage: Materials, methods and perspectives. Renew Sustain Energy Rev 2015;50:457–69.

[6] Jahangiri H, Bennett J, Mahjoubi P, Wilson K, Gu S. A review of advanced catalyst development for Fischer–Tropsch synthesis of hydrocarbons from biomass derived syngas. Catal Sci Technol 2014;4:2210–29.

[7] Jensen SH, Graves C, Mogensen M, Wendel C, Braun R, Hughes G, et al. Large-scale electricity storage utilizing reversible solid oxide cells combined with underground. Energy Environ Sci 2015;8:2471–9.

[8] Wendel CH, Kazempoor P, Braun RJ. Novel electrical energy storage system based on reversible solid oxide cells: System design and operating conditions. J Power Sources 2015;276:133–44.

[9] Rivera-Tinoco R, Farran M, Bouallou C, Auprêtre F, Valentin S, Millet P, et al. Investigation of power-to-methanol processes coupling electrolytic hydrogen production and catalytic CO_2 reduction. Int J Hydrogen Energy 2016;41:4546–59.

[10] Rönsch S, Schneider J, Matthischke S, Schlüter M, Götz M, Lefebvre J, et al. Review on methanation - From fundamentals to current projects. Fuel 2016;166:276–96.

[11] Ren J, Musyoka NM, Langmi HW, Mathe M, Liao S. Current research trends and perspectives on materials-based hydrogen storage solutions: A critical review. Int J Hydrogen Energy 2017;42:289–311.

[12] Chen B, Xu H, Zhang H, Tan P, Cai W, Ni M. A novel design of solid oxide electrolyser integrated with magnesium hydride bed for hydrogen generation and storage–A dynamic simulation study. Appl Energy 2017;200:260–72.

[13] Chan S, Low C, Ding O. Energy and exergy analysis of simple solid-oxide fuel-cell power systems. J Power Sources 2002;103:188–200.

[14] Mary N, Augustine C, Joseph S, Heartson S. Dynamic modeling and fuzzy control for solid oxide fuel cell (SOFC). Int J Adv Res Electr Electron Instrum Eng 2016;5:5488–97.

[15] Padulles J, Ault GW, Mcdonald JR. An integrated SOFC plant dynamic model for power systems simulation. J Power Sources 2000;86:495–500.

[16] Blackburn J, Reethof G, Shearer J. Fluid Power Control,(1960). MIT Press USA n.d.

[17] Gao Z, Mogni L V., Miller EC, Railsback JG, Barnett SA. A perspective on low-temperature solid oxide fuel cells. Energy Environ Sci 2016;9:1602–44.

[18] Schlereth D, Hinrichsen O. A fixed-bed reactor modeling study on the methanation of CO2. Chem Eng Res Des 2014;92:702–12.

[19] Froment GF. Methane Steam Reforming , Methanation and Water-Gas Shift : 1 . Intrinsic Kinetics 1989;35:88–96.

[20] Rostrup-Nielsen JR, Pedersen K, Sehested J. High temperature methanation. Sintering and structure sensitivity. Appl Catal A Gen 2007;330:134–8.

[21] Wagner W, Kretzschmar H-J. IAPWS industrial formulation 1997 for the thermodynamic properties of water and steam. Int Steam Tables Prop Water Steam Based Ind Formul IAPWS-IF97 2008:7–150.

[22] Koschany F, Schlereth D, Hinrichsen O. On the kinetics of the methanation of carbon dioxide on coprecipitated $NiAl(O)_X$. Appl Catal B Environ 2016;181:504–16.

[23] Rönsch S, Köchermann J, Schneider J, Matthischke S. Global Reaction Kinetics of CO and CO_2 Methanation for Dynamic Process Modeling. Chem Eng Technol 2016;39:208–18.

[24] Wendel CH, Kazempoor P, Braun RJ. A thermodynamic approach for selecting operating conditions in the design of reversible solid oxide cell energy systems. J Power Sources 2016;301:93–104.

[25] Yi Y, Smith TP, Brouwer J, Rao AD, Samuelsen GS. Simulation of a 220 kW hybrid SOFC gas turbine system and data comparison. In: Electrochemical society proceedings volume 2003–07;2003.
[26] Ando Y, Oozawa H, Mihara M, Irie H, Urashita Y, Ikegami T. Demonstration of SOFC-micro gas turbine (MGT) hybrid systems for commercialization. Mitsubishi Heavy Industr Tech Rev 2015;52(4).

Figures

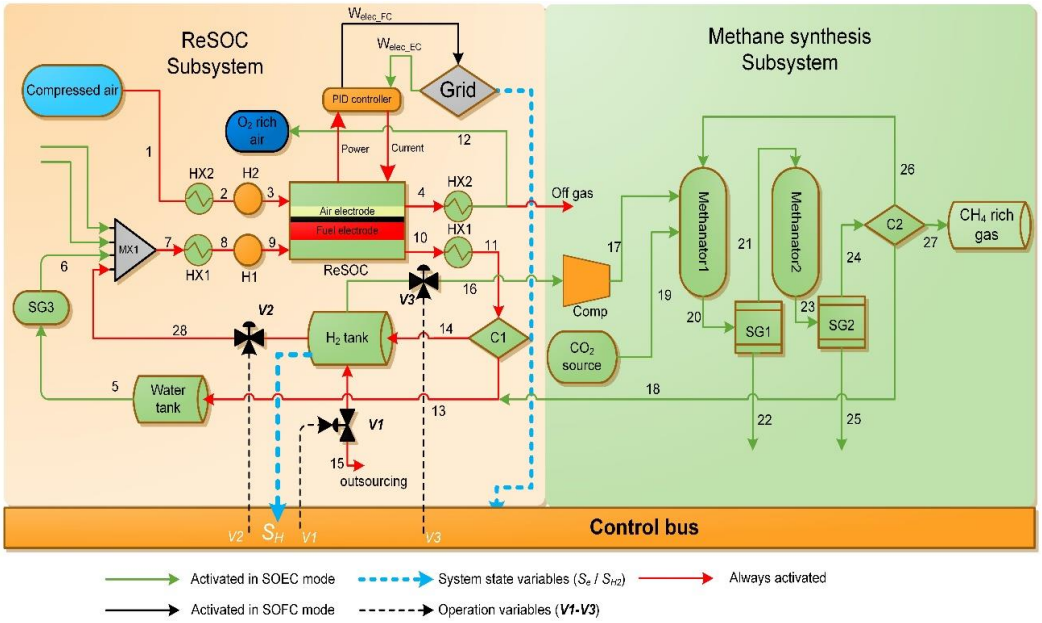

Fig. 1. The overall system schematic of the ReSOC-MS system.

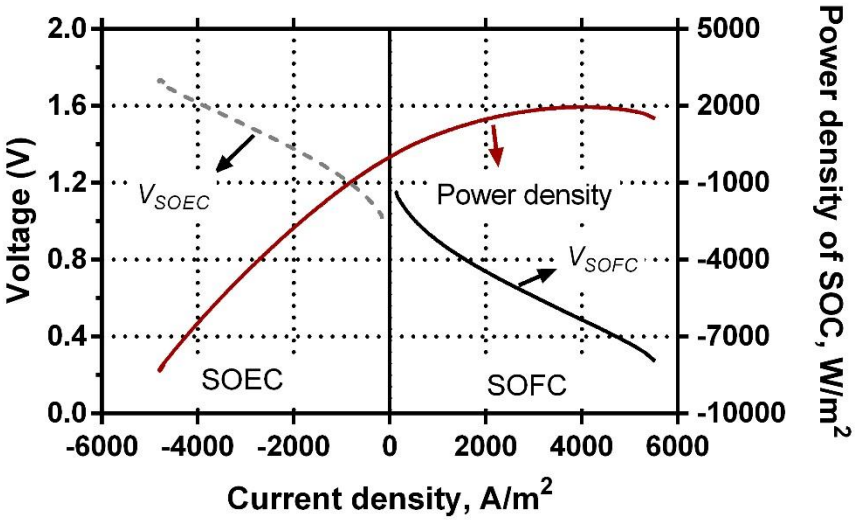

Fig. 2. The simulated ReSOC performance in dual modes: SOEC(left) and SOFC(right); Inlet fuel gas: 97% H_2, 3% H_2O at SOFC and 95% H_2O,5% H_2 at SOEC; Air electrode: air; 600 °C.

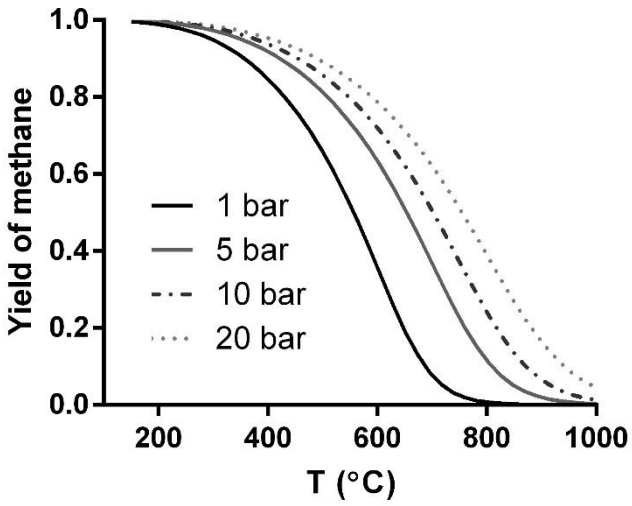

Fig. 3. Yield of methane at thermodynamic equilibrium for stoichiometric feed gas composition (CO_2 = 20%, H_2 = 80%) [10].

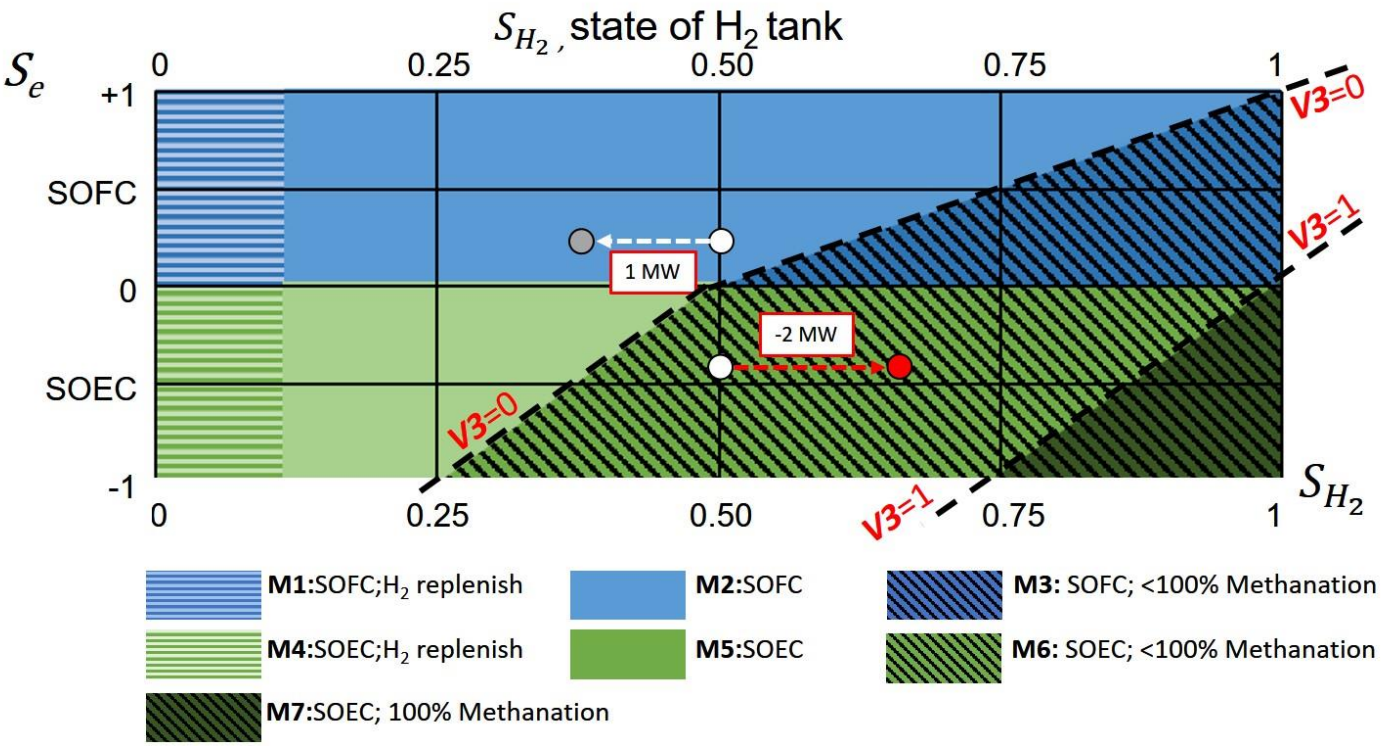

Fig. 4. Control strategy of 7 modes (**M1**–**M7**) depending on the system state and the stationary testing case state trajectory at 1 MW and −2 MW grid input.

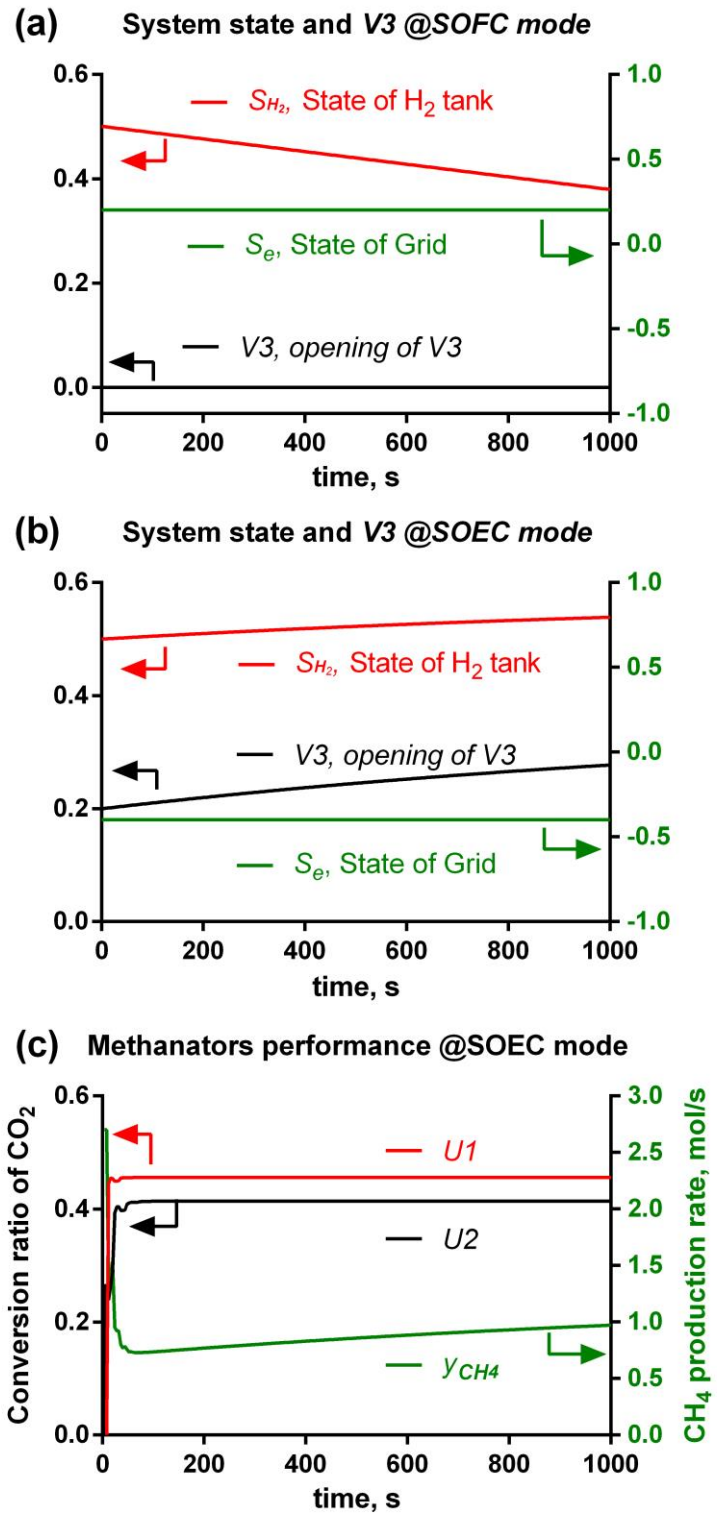

Fig. 5. S_e, S_{H_2} and ***V3*** in the stationary testing for 1000 s: (a) SOFC mode; (b) SOEC mode and (c) methanator performance at SOEC mode

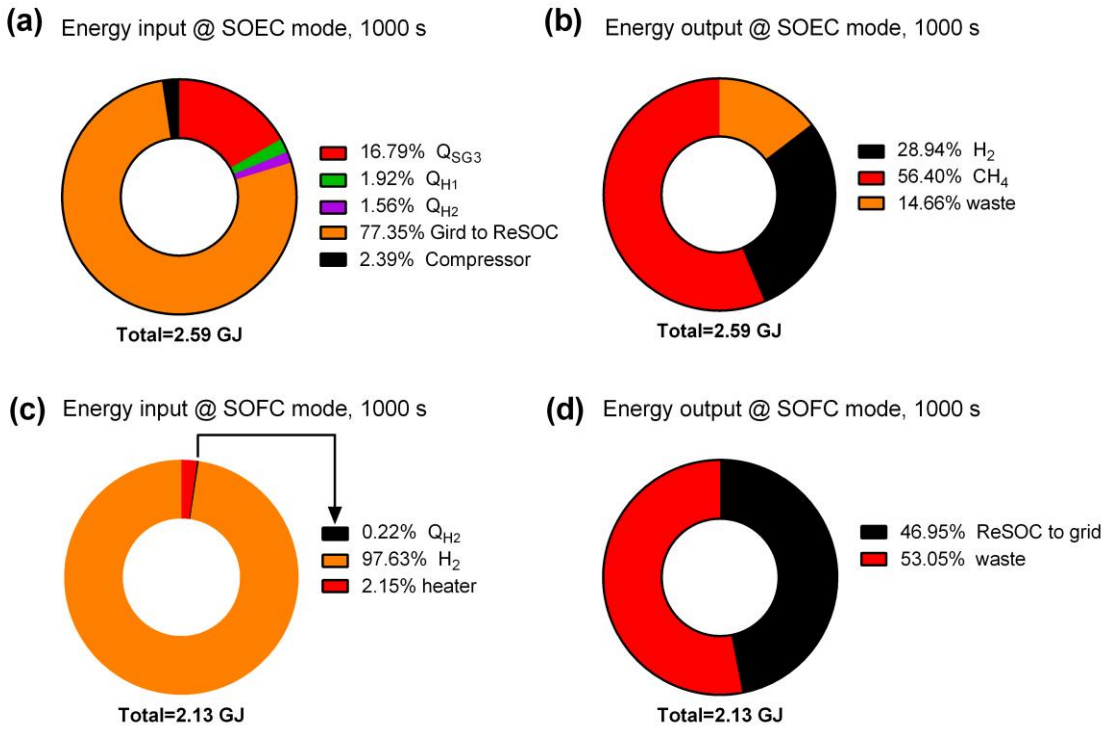

Fig. 6. Accumulative energy incomings and outgoings for the SOEC case (a–b) and SOFC case (c–d) at 1000 s.

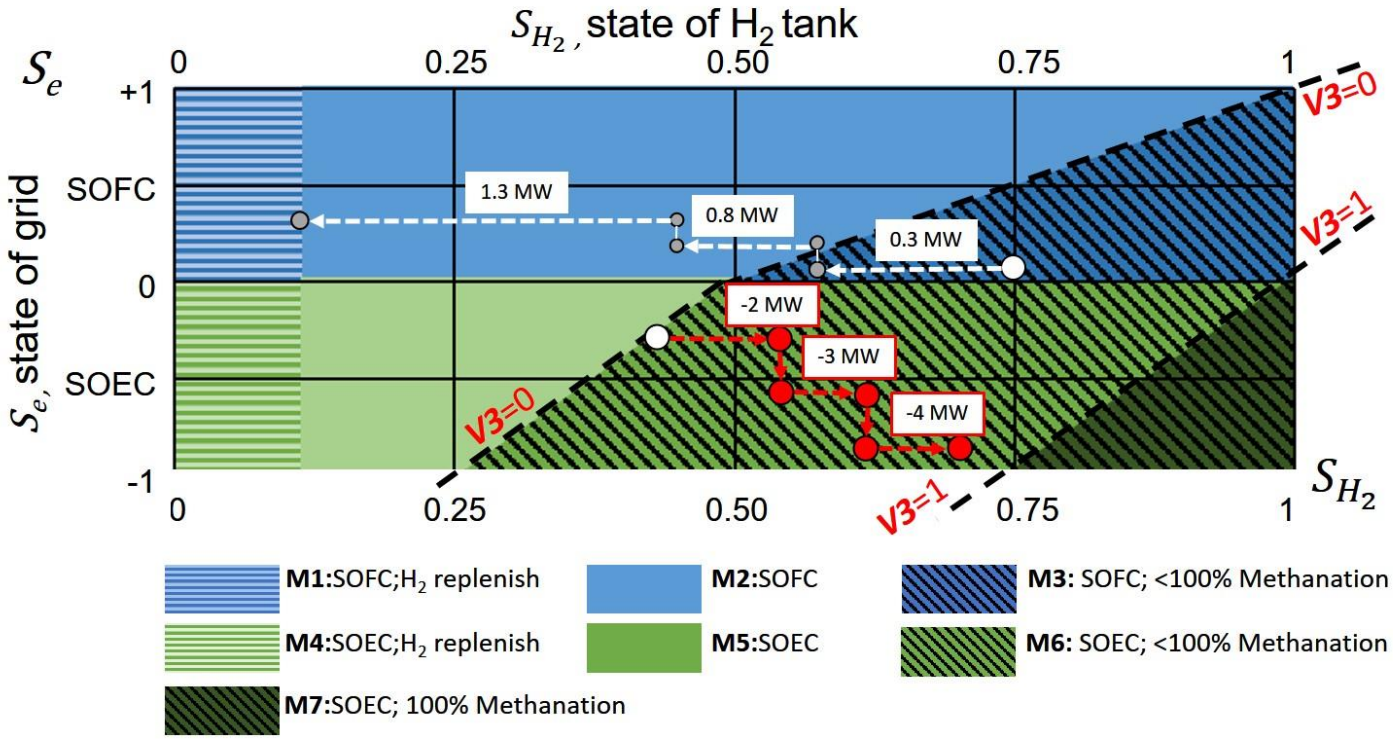

Fig. 7. The dynamic operation testing of SOEC and SOFC mode of the ReSOC-MS system and its system state trajectories (red arrow: SOEC; white arrow: SOFC).

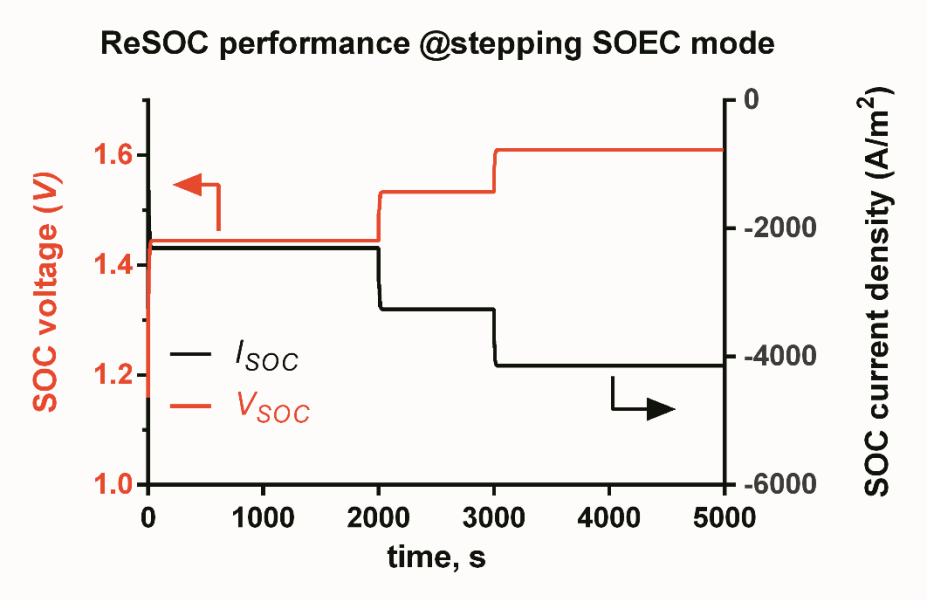

Fig. 8. Dynamic performance of the ReSOC at SOEC mode.

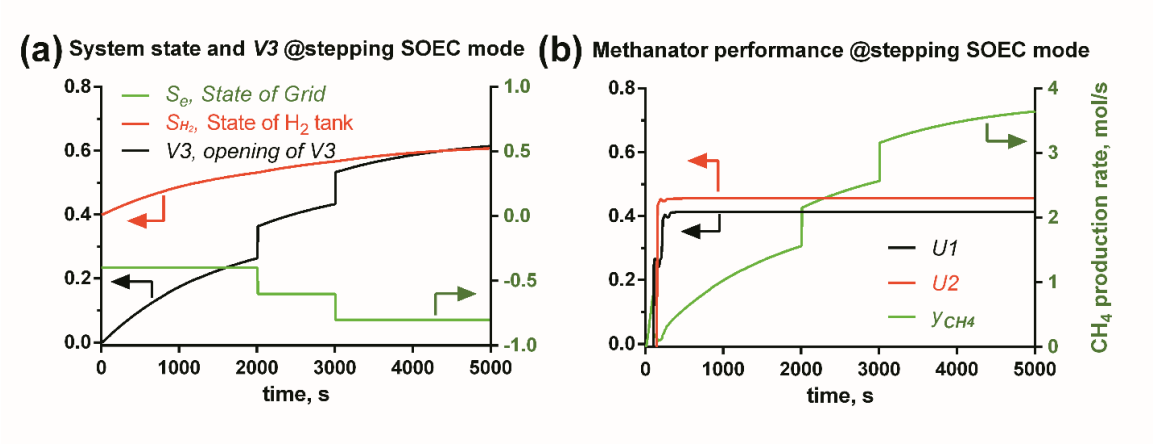

Fig. 9. (a) system state variables and (b) methanation system dynamic performance at stepping SOEC condition.

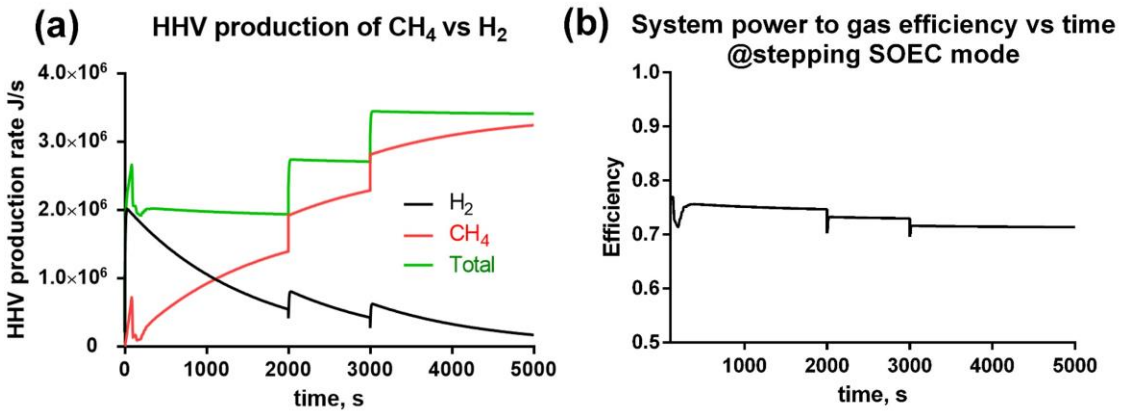

Fig. 10. (a) HHV of CH_4 and H_2 produced at the stepping SOEC condition; (b) the system power to gas efficiency at stepping SOEC condition.

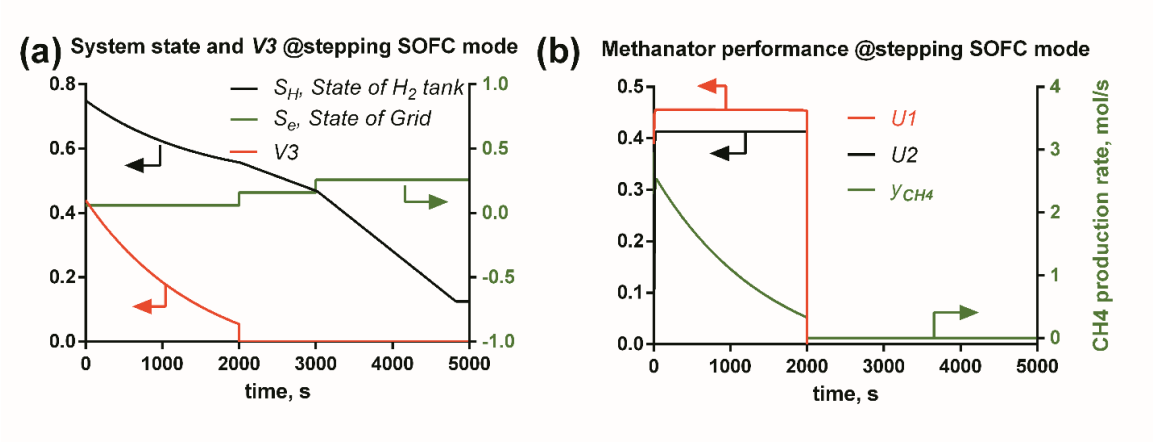

Fig. 11. (a) system state variables; (b) methanation system dynamic performance at stepping SOFC mode.

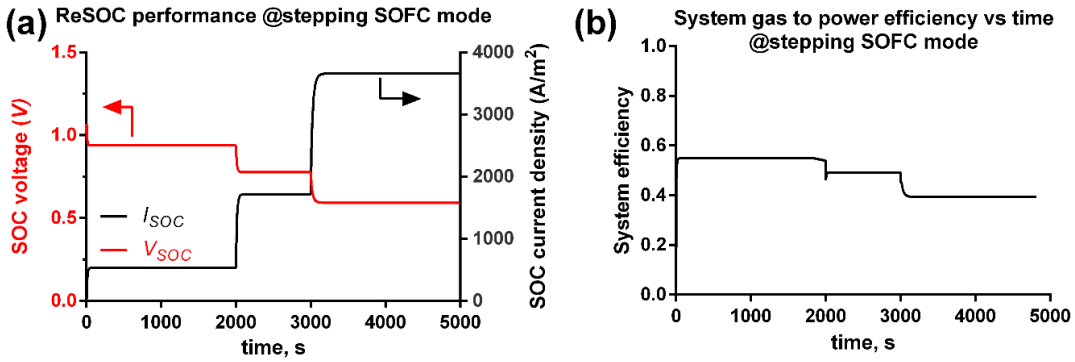

Fig. 12. (a) The current and voltage of ReSOC; (b) system gas to power efficiency dynamic performance at stepping SOFC mode.

Tables

Table 1 The nominal operation conditions of auxiliary blocks of the ReSOC subsystem.

Blocks	**Parameters and values**
Heat exchanger (***HX1***–***2***)	Effectiveness: 0.85
Heaters (***H1***–***2***)	Outlet temperature: 600 °C
Steam generator (***SG3***)	Outlet temperature: 100 °C
Compressed air	Flowrate: 0.5 mol s^{-1} at SOEC; $10 \cdot S_e$ mol s^{-1} at SOFC; Pressure: slightly[a]>1 bar
Water tank	25 °C, 1 bar
H_2 tank	25 °C, 1 bar, capacity: 6000 mol H_2
Maximum valve flowrate for ***V2*** and ***V3***	55 mol s^{-1}; 20 mol s^{-1}
Condenser (***C1***)	Condensing temperature: 100 °C
PID controller	kp = 0.0001; ki = 1; kd = 1

[a] ideally assumed to be 1 bar in simulation, while in practical, the outlet pressure of the compressed air tank should be calibrated at slightly > 1 bar to offset the pressure loss.

Table 2 Methanator design parameters used in the modelling [18].

Methanator parameters	**Value**
Working pressure	10 bar
Catalyst type	Ni/Al_2O_3
Catalyst density (ρ_c)	2800 kg mol^{-1}
Bed porosity	0.4
Methanator catalyst loading	3.0 kg
Methanator inner diameter	0.45 m
Methanator length	2.0 m
Space velocity, GSHV (nominal, ***V3*** = 1)	6800 h^{-1} (STP)
Inlet gas composition before mixing with recycled gas	H_2:CO_2 = 4
Inlet gas flowrate before mixing (nominal, ***V3*** =1)	25 mol s^{-1}
Discretized element number	400

Table 3 The operation parameters of auxiliary blocks of methanation subsystem.

Blocks	**Parameters**	**Value**
H_2 source (***S16***)	Temperature, T_{H_2}	25 °C
	Pressure, P_{H_2} [19]	10 bar
	Maximum flowrate, F_{H_2}	20 mol s^{-1}
CO_2 source	Temperature, T_{CO_2}	25 °C
	Pressure, P_{CO_2} [19]	10 bar
	Maximum flowrate, F_{CO_2}	5 mol s^{-1}
Steam generator (***SG1***–***2***)	Temperature of feed-water	25 °C
	Outlet steam temperature	100 °C
Methanator1	Inlet temperature	250 °C
Methanator2	Inlet temperature [20]	400 °C
Condenser (***C2***)	Recycle ratio	10%
	Outlet temperature at 10 bar [21]	177 °C
Compressor (***COMP***)	Compressing ratio	10
	Isentropic efficiency	85%

Table 4 Summary of stationary performance of the ReSOC-MS at SOFC mode and SOEC case.

Parameters	**SOFC case**	**SOEC case**
S_e input	0 s – 1000 s: 0.2 (1 MW)	0 s – 1000 s: −0.4 (−2 MW)
Operation time	1000 s	1000 s
Initial H_2 tank state, S_{H_2}	0.5	0.5
Total power output to grid , W_{g_SOFC}	1000 MJ	−2000 MJ
Total auxiliary power input, W_{aux_SOFC}	50.5 MJ	585.6 MJ
HHV value of H_2 consumption for SOFC, HHV_{H2_SOFC}	2079.5 MJ	Nil
Total HHV production of H_2 and CH_4, HHV_{fuel_SOEC}	Nil	2214 MJ
Average system efficiency	46.95% (gas to power)	85.34 % (power to gas)
Operating Voltage of ReSOC, V_{SOC}	0.71 V	1.44 V
Average methane production rate, y_{CH_4}	Nil	0.875 mol s^{-1}

Table 5 Summary of dynamic operation conditions and performance of the ReSOC-MS system in the SOEC case.

Performance parameters	**Value**
Average methane production rate, y_{CH_4}	2.2326 mol s^{-1}
Average CO_2 conversion ratio	$U1$ = 0.456; $U2$ = 0.41
Operation time	5000 s
Initial H_2 tank state, S_{H_2}	0.4
Stepping S_e input	0 s – 2000 s: −0.4 (−2 MW)
	2000 s – 3000 s: −0.6 (−3 MW)
	3000 s – 5000 s: −0.8 (−4 MW)
Total HHV production of H_2 and CH_4, HHV_{fuel_SOEC}	13482 MJ
Total grid electricity input: W_{g_SOEC}	15000 MJ
Total auxiliary power input, W_{aux_SOEC}	3968.7 MJ
Average system efficiency (power to gas)	71.70%
Operating voltage of ReSOC, V_{SOC}	1.44 V; 1.53 V; 1.61 V
Working temperature of ReSOC, T_{SOC}	600 °C

Table 6 Summary of dynamic operation conditions and performance of the ReSOC-MS system in the SOFC case.

Performance parameters	**Value**
Stepping S_e input	0 s – 2000 s: 0.06 (0.3 MW) 2000 s – 3000 s: 0.16 (0.8 MW) 3000 s – 5000 s: 0.26 (1.3 MW)
Operation time	5000 s
Initial H_2 tank state, S_{H_2}	0.75
Total grid power output, W_{g_SOFC}	3999 MJ
Total auxiliary power input, W_{aux_SOFC}	340.2 MJ
HHV value of H_2 consumption for SOFC, HHV_{H2_SOFC}	8366 MJ
Average system efficiency (gas to power)	46.1%
Operating voltage of ReSOC, V_{SOC}	0.938 V; 0.776 V; 0.592 V